Improved Bounds on Ultralight Scalar Dark Matter in the Radio-Frequency Range

Oleg Tretiak, Xue Zhang,* Nataniel L. Figueroa, and Dionysios Antypas
Johannes Gutenberg-Universität Mainz, 55128 Mainz, Germany
and Helmholtz-Institut, GSI Helmholtzzentrum für Schwerionenforschung, 55128 Mainz, Germany

Andrea Brogna
Johannes Gutenberg-Universität Mainz, 55128 Mainz, Germany

Abhishek Banerjee and Gilad Perez
Department of Particle Physics and Astrophysics, Weizmann Institute of Science, Rehovot 7610001, Israel

Dmitry Budker
Johannes Gutenberg-Universität Mainz, 55128 Mainz, Germany;
Helmholtz-Institut, GSI Helmholtzzentrum für Schwerionenforschung, 55128 Mainz, Germany
and Department of Physics, University of California, Berkeley, California 94720, USA

(Received 14 January 2022; accepted 2 June 2022; published 11 July 2022)

We present a search for fundamental constant oscillations in the range 20 kHz–100 MHz that may arise within models for ultralight dark matter (UDM). Using two independent optical-spectroscopy apparatuses, we achieve up to ×1000 greater sensitivity in the search relative to previous work [D. Antypas *et al.*, Phys. Rev. Lett. **123**, 141102 (2019).]. We report no observation of UDM and thus constrain respective couplings to electrons and photons within the investigated UDM particle mass range 8×10^{-11}–4×10^{-7} eV. The constraints significantly exceed previously set bounds from atomic spectroscopy and, as we show, may surpass in future experiments those provided by equivalence-principle (EP) experiments in a specific case regarding the combination of UDM couplings probed by the EP experiments.

DOI: 10.1103/PhysRevLett.129.031301

Introduction.—One of the important quests of modern physics is understanding the nature of dark matter. Within a broad class of scenarios, dark matter is made of bosonic fields that are associated with light particles such as axions or axionlike particles, which are classified according to their spin, interaction types with standard model (SM) matter, and resulting observables [1–4]. They may have mass m_ϕ in a broad range 10^{-22}–10 eV and form a classical oscillating field $\phi(t) \approx \phi_0 \sin(2\pi f_\phi t)$, with the oscillation frequency being close to the Compton frequency of the particle $f_\phi = m_\phi/2\pi$ [5]. In cases where this ultralight dark matter (UDM) field ϕ has scalar coupling to SM matter, the interaction is expected to appear as an apparent oscillation in the fundamental constants (FCs) occurring at the frequency f_ϕ. It may also give rise to equivalence-principle (EP)-violating acceleration [4,6]. Such scalar couplings are present within string and dilatonic theories [7] and within beyond-SM extensions introduced to explain the hierarchy problem [8] that were further developed to accommodate the presence of UDM [9–11].

Searches for effects of light scalar fields involve analysis of astrophysical data from the early Universe [12,13], fifth-force experiments to probe EP violation [14–17] or apparent FC oscillations. The latter give rise to oscillations of specific atomic parameters that can be sensitively probed. For instance, the energy of atomic levels and thus the frequency of electronic transitions is approximately proportional to the Rydberg constant $R_\infty = (1/2)m_e\alpha^2$, where m_e is the electron mass and α is the fine-structure constant. In addition, the length of solid bodies, which is proportional to the Bohr radius $\alpha_B = (\alpha m_e)^{-1}$ depends on the same constants. Atomic and optical techniques are sensitive means to look for oscillations in α and m_e [18], for example, by probing the frequencies of atomic transitions [7,22] in atomic clocks [23–26] and comparing these to the resonance frequency of optical cavities [27,28], via laser interferometry [29,30], comparison of two cavities [31], gravitational-wave detectors [32–34], and other methods [35,36].

A method involving optical spectroscopy of an atomic ensemble to probe oscillations of α and m_e in the radio-frequency (rf) range 20 kHz–100 MHz ($8 \times 10^{-11} < m_\phi < 4 \times 10^{-7}$ eV) was introduced in Ref. [37]. In this range, searches for EP-violating fifth forces have been more sensitive in exploring the scalar field. FC oscillations may be greatly enhanced, however, if there exist UDM halos that are gravitationally bound to Earth [38,39] or the Sun [38–40]. Such hypothetical halos may result in an enhanced local dark matter (DM) density and, correspondingly, to enhancement of FC oscillations. In such cases, the observability of the effects of the scalar UDM field may be greater in the case of FC-oscillation experiments compared to EP-violation ones. This is because an EP-violating fifth-force involves virtual exchange of a bosonic particle that is independent of UDM (see, for instance, [41]). There is another reason why direct UDM searches and EP tests can be considered complementary to each other: in part of the parameter space of UDM-SM couplings probed by EP tests, their sensitivity is reduced compared to direct searches [36], as we discuss below.

Here we present an improved search for scalar UDM within the same mass range (8×10^{-11}–4×10^{-7} eV) as that explored in [37]. Through the use of improved apparatuses and techniques, we achieve a substantially greater sensitivity in probing fast FC oscillations and obtain constraints on the couplings of the scalar field that are improved by up to $\times10^3$ with respect to [37]. The sensitivity also significantly exceeds that of the recently reported results from the colocated optical interferometers (the Fermilab Holometer) [42] that cover part of the parameter space addressed by our experiments.

Experimental principle.—The idea to probe FC oscillations is to compare the frequency of an atomic transition $f_{\rm at}$ to the frequency f_L of a laser field exciting it and look for relative variations $\delta f = f_{\rm at} - f_L$ [37,43]. With f_L tuned to excite the transition, $f_L \approx f_{\rm at}$, and such variations occur because $f_{\rm at}$ and f_L have different dependence on the FCs. The dependence of the frequency f_i on a constant g can be quantified through the coefficient $Q_g^i = d\ln f_i/d\ln g$ [44]. With this, one may write for the relative variation: $(\delta f/f)_g = (Q_g^{\rm at} - Q_g^L)(\delta g/g)$, or, including contributions from both constants α and m_e considered here,

$$\frac{\delta f}{f} = (Q_\alpha^{\rm at} - Q_\alpha^L)\frac{\delta\alpha}{\alpha} + (Q_{m_e}^{\rm at} - Q_{m_e}^L)\frac{\delta m_e}{m_e}, \qquad (1)$$

where $f = f_L \approx f_{\rm at}$. The frequency of the laser resonator is linear in the inverse resonator length: $f_L \propto 1/L \propto m_e\alpha$ [44]. In addition, the atomic frequency $f_{\rm at} \propto m_e\alpha^{2+\epsilon}$, where the parameter ϵ accounts for enhanced sensitivity to α variation due to relativistic effects [45]. For the Cs D2 line employed in this Letter, $\epsilon \approx 0.26$ [46]. Therefore, $Q_\alpha^{\rm at} = 2.26$, $Q_{m_e}^{\rm at} = 1$, and $Q_\alpha^L = Q_{m_e}^L = 1$.

Equation (1) quantifies the experimental sensitivity in the limit of low FC-oscillation frequency and implies, for example, no sensitivity to m_e oscillations since $Q_\alpha^L = Q_{m_e}^L$. However, the detection sensitivity to α or m_e is not uniform across the entire frequency range; one has to consider the response of atoms and the laser resonator to FC oscillations and distinguish different frequency ranges that are determined by the various experimental timescales. Indeed, the low-frequency limit (probed, for example, in [28]) is only one of the relevant ranges when probing rf oscillations [44,47], as in this case additional ranges become relevant. For instance, the f_L follows changes in the resonator length up to the acoustic cutoff frequency of the resonator f_{c1}, with $f_{c1} \approx 50$ kHz in our apparatus [37]. At frequencies higher than f_{c1}, f_L is independent of the FC oscillations. This transition in sensitivity can be incorporated through a response function $h_L(f_\phi)$, with $h_L(f_\phi) = 1$ below f_{c1} and $h_L(f_\phi) = 0$ above f_{c1}. In addition, the $f_{\rm at}$ is primarily sensitive to FC oscillations up to frequency f_{c2} equal to the observed transition linewidth Γ. This atomic response can be characterized through the function $h_{\rm at}(f_\phi)$, with $h_{\rm at}(f_\phi)\to 1$ for $f_\phi \ll f_{c2}$ and $h_{\rm at}(f_\phi)\to 0$ for $f_\phi \gg f_{c2}$. In practice, $h_{\rm at}(f_\phi)$ is determined through apparatus calibration. Inserting these response functions and the respective values of coefficients Q_g into Eq. (1), one obtains

$$\frac{\delta f}{f} = [2.26h_{\rm at}(f_\phi) - h_L(f_\phi)]\frac{\delta\alpha}{\alpha} + [h_{\rm at}(f_\phi) - h_L(f_\phi)]\frac{\delta m_e}{m_e}. \qquad (2)$$

We see that $\delta f/f = 1.26\delta\alpha/\alpha$ in the limit of low frequency $f_\phi < f_{c1}$, and $\delta f/f = 2.26\delta\alpha/\alpha + \delta m_e/m_e$ at intermediate frequencies $f_{c1} < f_\phi < f_{c2}$, while $\delta f/f \to 0$ in the limit of high frequency $f_\phi \gg f_{c2}$.

If the FC oscillations arise due to scalar UDM, their amplitude will be associated with couplings of the oscillatory UDM field to SM matter. This field is expected to exhibit stochastic amplitude fluctuations on a timescale equal to its oscillation coherence time τ_c [48]. For measurement time $T \gg \tau_c$ (which is true for the Galactic halo case, where τ_c is in a range of 10 ms–55 s), this stochasticity can be neglected. The field acquires a deterministic amplitude and is given by $\phi(t) \approx m_\phi^{-1}\sqrt{2\rho_{\rm DM}}\sin(m_\phi t)$ [10], where $\rho_{\rm DM} \approx 3\times10^{-6}$ eV^4 is the estimated local Galactic density of DM [49]. Within the field, the constants acquire a small, time-dependent amplitude, such that

$$\alpha(t) = \alpha_0[1 + g_\gamma\phi(t)], \qquad (3)$$

$$m_e(t) = m_{e,0}\left[1 + \frac{g_e}{m_{e,0}}\phi(t)\right], \qquad (4)$$

where g_γ and g_e are coupling constants of UDM to the photon and the electron, and a_0 and $m_{e,0}$ are the SM fine-structure constant and electron mass, respectively. One can make use of Eq. (2) to relate an observed variation $\delta f/f$ to the couplings g_γ and g_e,

$$\frac{\delta f}{f} = \begin{cases} 1.26 g_\gamma m_\phi{}^{-1}\sqrt{2\rho_{\rm DM}}h_{\rm at}(f_\phi), & f_\phi \le f_{c1} \\ \left(2.26 g_\gamma + \frac{g_e}{m_{e,0}}\right) m_\phi{}^{-1}\sqrt{2\rho_{\rm DM}}h_{\rm at}(f_\phi), & f_\phi > f_{c1}, \end{cases} \quad (5)$$

where the atomic response $h_{\rm at}(f_\phi)$ is to be determined experimentally. In the low-frequency limit, there is no sensitivity to g_e, while above the acoustic cutoff f_{c1} there is sensitivity to both g_e and g_γ couplings. In the absence of an observation of FC oscillations, Eq. (5) can be used to place bounds on g_e and g_γ, as it was done in [37].

Apparatus, data acquisition, and analysis.—The experiment was designed to address the principal limiting factor of the previous work [37] by introducing a more advanced data acquisition system. In addition, we implemented two different realizations of the setup in order to better control for spurious UDM signatures. The two setups (apparatuses A and B) are described in the Supplemental Material [50].

Apparatus A is a new version of the Cs Doppler-free polarization spectroscopy setup [37]. The improvements include (a) using a stronger transition $6^2S_{1/2}(F=4) \rightarrow 6^2P_{3/2}(F=5)$, (b) increased laser-beam size and power to improve signal-to-shot-noise ratio, and (c) employing a graphics card to calculate and average card to efficiently process recorded data, in parallel with the data acquisition process. The new apparatus features a nearly 100% measurement duty cycle and can reach better statistical sensitivity in search for UDM than that in Ref. [37] in less than 1 s (the experiment described in [37] took 66 h in total).

Apparatus B was built independently of apparatus A. It makes use of a different laser source and implements Doppler-broadened spectroscopy on the $F=4 \rightarrow F'=3$, 4, 5 components of the Cs D2 line. This extends the bandwidth for the search for FC oscillations up to more than 100 MHz. The data acquisition system samples the experimental signal at a lower rate compared to that in apparatus A, resulting in a lower sensitivity; however, this system is more immune to parasitic technical noise. (See Supplemental Material [50] for detailed apparatus description, which includes Refs. [51,52]).

In both experiments, sensitivity to FC oscillations is enabled by tuning the laser in frequency to excite the respective atomic resonance. The spectroscopy signal is recorded in 1.1- and 0.1-s-long intervals for experiments A and B, respectively, and corresponding power spectra are continuously computed and averaged. These are subsequently investigated for FC oscillations, which are expected to appear as excess power in the spectra.

In apparatus A we averaged 628 700 power spectra corresponding to ≈187 h of pure acquisition time. Because of high resolution and statistical sensitivity, many thousands of spurious peaks are present in the resulting spectrum. The realization of apparatus A does not allow us to eliminate them and we cannot establish a good UDM candidate exclusion at these points. Most of these peaks come from frequency modulation of the laser light, which is most probably the result of electromagnetic interference with a switching power supply (they form groups with peaks spaced by 20 Hz). In this Letter, we present this apparatus as an ultimately sensitive device that requires some further design improvement in experimental technique as well as in data analysis [50].

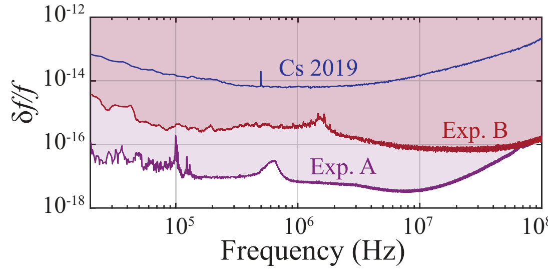

FIG. 1. Constraints on the fractional frequency oscillations $\delta f/f$, shown for experiments A and B at the 95% C.L., alongside constraints from the earlier work [37]. While generally more sensitive, experiment A is not directly used for obtaining new constraints due to the presence of spurious peaks (see text).

In apparatus B, we acquired data for a total of 113 h, realizing an ≈16% duty cycle. We alternated acquisition with the laser frequency tuned either on or off the optical transition (where there is no sensitivity to FC oscillations), resulting in pure integration of 9 h in each case. This mixed data taking allows subtraction of the on- and off-resonance spectra, and elimination of most of the signals are not due to UDM. However, a total of 70 peaks remained in the subtracted spectrum with power exceeding a threshold for FC-oscillation detection at the 95% confidence level (C.L.). These were primarily due to apparatus pickup or due to parasitic laser frequency or amplitude noise. We investigated them using different methods. For example, we did dedicated runs to check peaks that were nearly eliminated in the main run and eventually observed residual power for these below the detection threshold. In addition, we took advantage of the in-tandem experiments to cross-check spurious UDM candidates. Several peaks in the spectrum of B, were either absent in A, or had corresponding power significantly smaller than the detection threshold in B, allowing elimination. Eventually, within the sensitivity of B we found no possible signatures of FC oscillations.

We show resulting $\delta f/f$ constraints in Fig. 1, produced with consideration of the "look elsewhere" effect [53] for the $N \approx 1.1 \times 10^8$ and $N \approx 1.6 \times 10^6$ frequency bins in the power spectra of A and B, respectively. We note that the shown limits from A represent the ultimate apparatus sensitivity. This is likely achievable via a future implementation of a dual on- and off-resonance acquisition and cross-comparison of data with those from another, independent setup of similar sensitivity. (See Supplemental Material for the data processing details, spurious peak

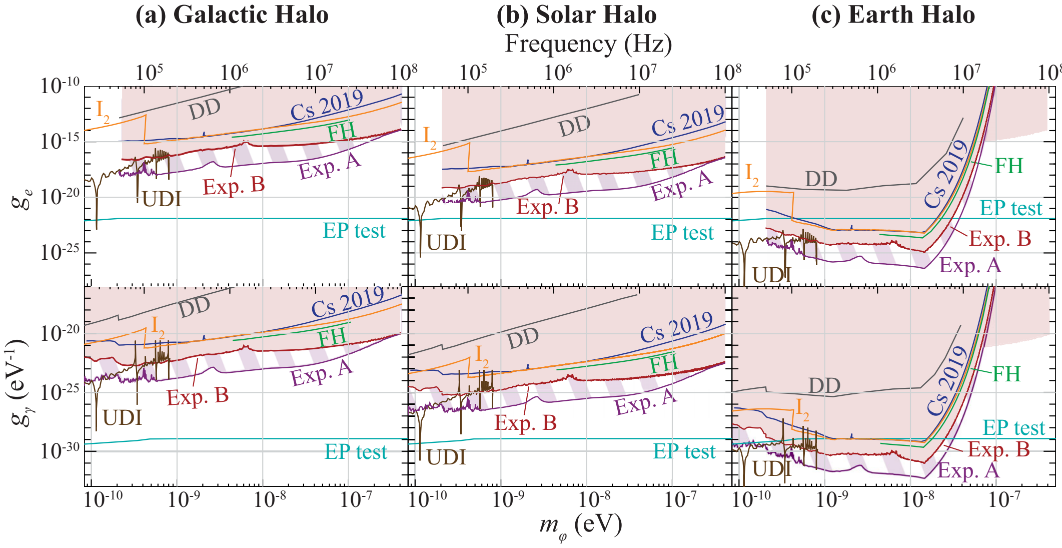

FIG. 2. Exclusion plots at the 95% C.L. for the coupling to the electron mass (top) and the fine-structure constant (bottom), produced within the Galactic (a), solar (b), and Earth (c) halo UDM scenarios. The constraint on g_e is only shown for $f > f_{c1} \approx 50$ kHz, [see Eq. (5)]. Also shown are constraints from the previous work (Cs 2019) [37], iodine spectroscopy (I_2) [36], an experiment using dynamic decoupling (DD) [27], an unequal-delay interferometer (UDI) [35], the Fermilab Holometer (FH) [42], and EP tests [14,15]. The exclusion regions for the Galactic halo are also shown on the plot for the hypothetical Earth halo scenario, since these are stronger for the larger-mass region. The plots for experiment A are shown for reference and are not actual constraints (see text and Supplemental Material [50]).

elimination strategy, sensitivity losses due to scalloping, and DM decoherence effects [50], which includes Refs. [54–58].)

Constraints on UDM couplings.—In the absence of detection of FC oscillations, we use the $\delta f/f$ constraints of experiment B (Fig. 1) and apply Eq. (5) to set upper bounds on the UDM couplings to the electron mass g_e and fine-structure constant g_γ, respectively. In addition, to illustrate the potential of our method in probing UDM, we consider constraints computed using the $\delta f/f$ limits, which may be ultimately feasible with experiment A (Fig. 1).

We show bounds for the case of the standard Galactic UDM halo scenario ($\rho_{\rm DM} \approx 3 \times 10^{-6}$ eV^4 [49]) in Fig. 2(a). To derive these, we assume that FC oscillations arise due to a single coupling to either g_e or g_γ and incorporate a correction to account for degradation in sensitivity in the high end of the investigated frequency range, due to the finite coherence of the UDM field (Q factor of $\approx 1.1 \times 10^6$ within the Galactic halo scenario).

The couplings g_e and g_γ can be further constrained within scenarios assuming the presence of an UDM halo that is gravitationally bound around the Sun [40] or Earth [38]. Within these scenarios, the UDM field has increased Q factor, which is, respectively, $\approx 9 \times 10^7$ and ∞. Relative to the standard Galactic halo density, the UDM density is enhanced by up to $\times 10^5$ for the solar halo. For an Earth halo, the possible enhancement is strongly dependent on UDM particle mass. We show limits from consideration of these models in Figs. 2(b) and 2(c).

An UDM field may couple to several species of the SM (this is indeed the case in the two concrete natural realization of scalar UDM that were considered in the literature, either as a dilaton field [7] or an axion subject to double breaking of the shift symmetry [9,10]). Thus, an UDM model can be described via a coupling “vector” of five independent directions, $\vec{d} = d_{\alpha, m_e, \Lambda_{\rm QCD}, (m_u+m_d)/2, m_d - m_u}$ in a five-dimensional space, and a vector $\vec{Q}$ to quantify the respective sensitivity coefficients of any experiment. As noted in [36], the bounds arising from the direct UDM searches and EP tests are complementary to each other in this abstract space of coupling. Consequently, one can find a direction $\hat{Q}^{\perp}_{\rm Full}(m_\phi)$ in the five-dimensional parameter space that is orthogonal to the best four EP test bounds for a given DM particle mass. In our region of interest, $\hat{Q}^{\perp}_{\rm Full}(m_\phi)$ is chosen as follows: below mass 5×10^{-9} eV it is orthogonal to the EP tests comparing two test bodies made out of Be-Al [59], Be-Ti [15], Cu-Pb [14], and Be-Cu [60] and written as $\hat{Q}^{\perp}_{\rm Full}(m_\phi) \simeq (0.003, -0.987, 0.002, -0.001, -0.162)$; above 5×10^{-9} eV it is orthogonal to the Be-Al, Be-Ti, Cu-Pb, and Cu-Pb alloy [61] EP tests and can be given as $\hat{Q}^{\perp}_{\rm Full}(m_\phi) \simeq (0.020, 0.983, 0.018, -0.010, 0.178)$. This choice of $\hat{Q}^{\perp}_{\rm Full}(m_\phi)$ is the same as that discussed in [36]. What is interesting is that $\hat{Q}^{\perp}_{\rm Full}(m_\phi)$ has a sizable overlap with the direction of the electron coupling d_{m_e}, which makes experiments looking for FC oscillations particularly competitive for searches in this particular direction in coupling space.

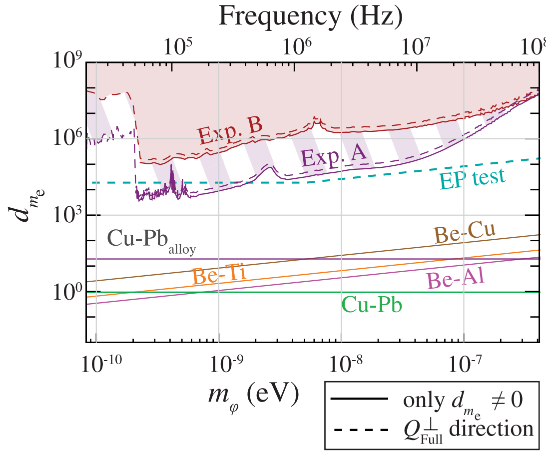

FIG. 3. Exclusion plot for d_{m_e} at the 95% C.L.; the solid lines assume a model where only $d_{m_e} \neq 0$. The dashed lines depict the bounds for a model defined by a vector of coupling defined by $\hat{Q}^{\perp}_{\rm Full}(m_\phi)\cdot\vec{d}$, that is, orthogonal to the sensitivities of four leading EP test experiments projected onto d_{m_e}. The bound from the fifth-best EP test experiment (whose sensitivity on the second model projected onto the d_{m_e} direction, is shown by the dashed turquoise line. This illustrates that there is a variant of theory, where the present experiments can rival the limits from EP tests. The plots for experiment A are shown for reference and are not actual constraints (see text and Supplemental Material [50]).

Figure 3 shows bounds for the coupling to m_e along the direction $\hat{Q}^{\perp}_{\rm Full}(m_\phi)$. (For consistency with [36], we reexpress it in terms of the dimensionless constant $d_{m_e} = g_e M_{\rm Pl}/m_{e,0}$, where $M_{\rm Pl} = \sqrt{\hbar c/(8\pi G_N)} = 2.4\times 10^{18}\,{\rm GeV}$ is the Planck mass.) For comparison, we additionally show constraints from our direct UDM searches and EP tests, assuming DM coupling to electrons only. We see that, in the direction $\hat{Q}^{\perp}_{\rm Full}(m_\phi)$, the direct search may ultimately approach (or surpass) the sensitivity level of EP tests. In this direction, the present experiment A shows the potential of future direct UDM searches that can be used to probe parameter space unconstrained by EP tests.

Focusing on a special direction in the multidimensional space that is orthogonal to the parameter space probed by EP tests represents a "tuning" of the model (or the direction of $\hat{Q}^{\perp}_{\rm Full}$) at the level of roughly $1:10^3$, however, we still find it interesting as follows. First, it highlights the value of pursuing different experimental approaches in parallel, as it is possible that our current theoretical biases are wrong and "nature" chose this direction out of coincidence or just from other unknown theoretical reasoning (for analogous discussion see, e.g., [62–67], among many other works). Second, we would like to quantify the level of tuning and fine-tuning (*à la* 't Hooft [68]) required to define this model. Among the five-dimensional parameter space, three ($d_{m_e,(m_u+m_d)/2,m_d-m_u}$) are technically natural and thus are radiatively stable, while $d_{\alpha,\Lambda_{\rm QCD}}$ are subjected to additive contributions. However, as mentioned above, in natural UDM models of the type of [7,10], these additive contributions are under control at least to leading order by construction. We can quantify the extra fine-tuning by looking at how much the presence of one coupling feeds into the other spoiling the delicate tuning. As the theory is perturbative, we can simply estimate as arising from one loop contribution, for instance (omitting for simplicity logarithmic terms) $\Delta d_\alpha \sim d_{m_e}\alpha/4\pi = \mathcal{O}(10^{-3})d_{m_e}$, which implies only mild or no tuning. Similar conclusions apply to the strong sector upon replacing d_α with $d_{\Lambda_{\rm QCD}}$ as long as the scale that set the dark model coupling is larger than a few GeV. (Note that, if the scale is below GeV, the coupling to $\Lambda_{\rm QCD}$ does not receive any radiative correction.)

Conclusion.—The present results represent a sensitivity improvement in the direct search for ultralight scalar dark matter of up to 3 orders of magnitude with respect to earlier work [69].

The sensitivity of the experiment is limited by our ability to suppress spurious noise; it might be possible to improve it by careful design of electronics and better electromagnetic shielding. Other future improvements may include designing an off-on resonance subtraction scheme in the higher-sensitivity experiment A analogous to the one successfully implemented in experiment B to suppress spurious spectral peaks. More importantly, both experiments together show that comparing two (or more) independent setups could be an efficient way to suppress spurious peaks. Statistical sensitivity in these setups can be further increased by scaling up the vapor cell diameter, by an order of magnitude, with reasonable size of components and measurement time. To obtain an optimal single-apparatus sensitivity in the whole investigated frequency range, one may employ both a narrow and a broad spectral line. Using other atoms with higher sensitivity to changes in FC, e.g., Yb [26], may yield another order of magnitude, possibly at the expense of additional complexity in the setup. Molecular spectroscopy makes the experiment sensitive to variation in nuclear mass [36,43].

On the side of the theoretical interpretation, the existence of the special "tuned" directions in the parameter space, where the present searches outperform EP tests, highlights the importance of pursuing different experimental approaches in parallel.

The authors gratefully acknowledge A. Garcon, D. Kanta, and P. Otte for help with the project and V. V. Flambaum and V. Dzuba for evaluating the relativistic corrections. A. B. thanks the Johannes Gutenberg University of Mainz for the hospitality and the Helmholtz Institute of Mainz for partial support during the completion of this work. This work was supported by the Cluster of Excellence "Precision Physics, Fundamental Interactions, and Structure of Matter" (PRISMA+ EXC 2118/1) funded by the German Research Foundation (DFG) within the German Excellence Strategy (Project

ID 39083149), by the European Research Council (ERC) under the European Union Horizon 2020 research and innovation program (project Dark-OST, Grant Agreement No. 695405), and Starting Grant (Grant Agreement No. 947696) by the DFG Reinhart Koselleck project, and by Internal University Research Funding of Johannes Gutenberg-University Mainz. The work of A. B. is supported by the Azrieli Foundation. The work of G. P. is supported by grants from U.S.-Israel Binational Science Foundation (BSF)-U.S. National Science Foundation (NSF) cooperation (No. 2019760), Friedrich Wilhelm Bessel research award, German-Israeli Foundation (GIF), the Israel Science Foundation (ISF) (Grant No. 718/18), Minerva, SABRA-Yeda-Sela-WRC Program, the Estate of Emile Mimran, and the Maurice and Vivienne Wohl Endowment.

*xuezhang@uni-mainz.de

[1] J. Preskill, M. B. Wise, and F. Wilczek, Phys. Lett. **120B**, 127 (1983).
[2] L. Abbott and P. Sikivie, Phys. Lett. **120B**, 133 (1983).
[3] M. Dine and W. Fischler, Phys. Lett. **120B**, 137 (1983).
[4] P. W. Graham, D. E. Kaplan, J. Mardon, S. Rajendran, and W. A. Terrano, Phys. Rev. D **93**, 075029 (2016).
[5] We use natural units, where $\hbar = c = 1$.
[6] A. Hees, O. Minazzoli, E. Savalle, Y. V. Stadnik, and P. Wolf, Phys. Rev. D **98**, 064051 (2018).
[7] A. Arvanitaki, J. Huang, and K. Van Tilburg, Phys. Rev. D **91**, 015015 (2015).
[8] P. W. Graham, D. E. Kaplan, and S. Rajendran, Phys. Rev. Lett. **115**, 221801 (2015).
[9] T. Flacke, C. Frugiuele, E. Fuchs, R. S. Gupta, and G. Perez, J. High Energy Phys. 06 (2017) 050.
[10] A. Banerjee, H. Kim, and G. Perez, Phys. Rev. D **100**, 115026 (2019).
[11] A. Banerjee, H. Kim, O. Matsedonskyi, G. Perez, and M. S. Safronova, J. High Energy Phys. 07 (2020) 153.
[12] Y. V. Stadnik and V. V. Flambaum, Phys. Rev. Lett. **115**, 201301 (2015).
[13] S. Sibiryakov, P. Sørensen, and T.-T. Yu, J. High Energy Phys. 12 (2020) 075.
[14] G. L. Smith, C. D. Hoyle, J. H. Gundlach, E. G. Adelberger, B. R. Heckel, and H. E. Swanson, Phys. Rev. D **61**, 022001 (1999).
[15] S. Schlamminger, K.-Y. Choi, T. A. Wagner, J. H. Gundlach, and E. G. Adelberger, Phys. Rev. Lett. **100**, 041101 (2008).
[16] P. Touboul *et al.*, Phys. Rev. Lett. **119**, 231101 (2017).
[17] J. Bergé, P. Brax, G. Métris, M. Pernot-Borràs, P. Touboul, and J.-P. Uzan, Phys. Rev. Lett. **120**, 141101 (2018).
[18] Other methods involve use of mechanical [19,20] or acoustic resonators [21].
[19] A. Arvanitaki, S. Dimopoulos, and K. Van Tilburg, Phys. Rev. Lett. **116**, 031102 (2016).
[20] J. Manley, D. J. Wilson, R. Stump, D. Grin, and S. Singh, Phys. Rev. Lett. **124**, 151301 (2020).
[21] W. M. Campbell, B. T. McAllister, M. Goryachev, E. N. Ivanov, and M. E. Tobar, Phys. Rev. Lett. **126**, 071301 (2021).
[22] M. S. Safronova, Ann. Phys. (Amsterdam) **531**, 1800364 (2019).
[23] K. Van Tilburg, N. Leefer, L. Bougas, and D. Budker, Phys. Rev. Lett. **115**, 011802 (2015).
[24] A. Hees, J. Guéna, M. Abgrall, S. Bize, and P. Wolf, Phys. Rev. Lett. **117**, 061301 (2016).
[25] P. Wcisło *et al.*, Sci. Adv. **4**, eaau4869 (2018).
[26] M. S. Safronova, S. G. Porsev, C. Sanner, and J. Ye, Phys. Rev. Lett. **120**, 173001 (2018).
[27] S. Aharony, N. Akerman, R. Ozeri, G. Perez, I. Savoray, and R. Shaniv, Phys. Rev. D **103**, 075017 (2021).
[28] C. J. Kennedy, E. Oelker, J. M. Robinson, T. Bothwell, D. Kedar, W. R. Milner, G. E. Marti, A. Derevianko, and J. Ye, Phys. Rev. Lett. **125**, 201302 (2020).
[29] Y. V. Stadnik and V. V. Flambaum, Phys. Rev. Lett. **114**, 161301 (2015).
[30] Y. V. Stadnik and V. V. Flambaum, Phys. Rev. A **93**, 063630 (2016).
[31] A. A. Geraci, C. Bradley, D. Gao, J. Weinstein, and A. Derevianko, Phys. Rev. Lett. **123**, 031304 (2019).
[32] A. Arvanitaki, P. W. Graham, J. M. Hogan, S. Rajendran, and K. Van Tilburg, Phys. Rev. D **97**, 075020 (2018).
[33] H. Grote and Y. V. Stadnik, Phys. Rev. Research **1**, 033187 (2019).
[34] S. M. Vermeulen *et al.*, Nature (London) **600**, 424 (2021).
[35] E. Savalle, A. Hees, F. Frank, E. Cantin, P.-E. Pottie, B. M. Roberts, L. Cros, B. T. McAllister, and P. Wolf, Phys. Rev. Lett. **126**, 051301 (2021).
[36] R. Oswald, A. Nevsky, V. Vogt, S. Schiller, N. L. Figueroa, K. Zhang, O. Tretiak, D. Antypas, D. Budker, A. Banerjee, and G. Perez, arXiv:2111.06883 [Phys. Rev. Lett. (to be published)].
[37] D. Antypas, O. Tretiak, A. Garcon, R. Ozeri, G. Perez, and D. Budker, Phys. Rev. Lett. **123**, 141102 (2019).
[38] A. Banerjee, D. Budker, J. Eby, H. Kim, and G. Perez, Commun. Phys. **3**, 1 (2020).
[39] A. Banerjee, D. Budker, J. Eby, V. V. Flambaum, H. Kim, O. Matsedonskyi, and G. Perez, J. High Energy Phys. 09 (2020) 004.
[40] N. B. Anderson, A. Partenheimer, and T. D. Wiser, arXiv:2007.11016.
[41] M. E. Peskin and D. V. Schroeder, *An Introduction to Quantum Field Theory* (Addison-Wesley, Reading, MA, 1995).
[42] L. Aiello, J. W. Richardson, S. M. Vermeulen, H. Grote, C. Hogan, O. Kwon, and C. Stoughton, Phys. Rev. Lett. **128**, 121101 (2022).
[43] D. Antypas, O. Tretiak, K. Zhang, A. Garcon, G. Perez, M. G. Kozlov, S. Schiller, and D. Budker, Quantum Sci. Technol. **6**, 034001 (2021).
[44] M. G. Kozlov and D. Budker, Ann. Phys. (Berlin) **531**, 1800254 (2019).
[45] V. V. Flambaum and V. Dzuba, Can. J. Phys. **87**, 25 (2009).
[46] V. Dzuba and V. V. Flambaum (private communication).
[47] D. Antypas, D. Budker, V. V. Flambaum, M. G. Kozlov, G. Perez, and J. Ye, Ann. Phys. (Berlin) **532**, 1900566 (2020).
[48] G. P. Centers, J. W. Blanchard, J. Conrad, N. L. Figueroa, A. Garcon, A. V. Gramolin, D. F. J. Kimball, M. Lawson, B. Pelssers, J. A. Smiga, A. O. Sushkov, A. Wickenbrock, D.

Budker, and A. Derevianko, Nat. Commun. **12**, 7321 (2021).

[49] *The Search for Ultralight Bosonic Dark Matter*, edited by D. F. Jackson Kimball and K. van Bibber (Springer, New York, 2021).

[50] See Supplemental Material at http://link.aps.org/supplemental/10.1103/PhysRevLett.129.031301 for a technical description of the raw-data file, which can be downloaded for analysis at https://irods-web.zdv.uni-mainz.de/irods-rest/rest/fileContents/zdv/project/m2_him_exp/mam/2022_dark_matter_v2/ExperimentA_data.dat?ticket=XD07Jrg8eBae4b7.

[51] P. Tremblay and R. Ouellet, in *Conference on Precision Electromagnetic Measurements* (IEEE, New York, 1990), pp. 252–253.

[52] Y. Torii, H. Tashiro, N. Ohtsubo, and T. Aoki, Phys. Rev. A **86**, 033805 (2012).

[53] J. D. Scargle, Astrophys. J. **263**, 835 (1982).

[54] L. Sevgi, IEEE Antennas Propag. Mag. **49**, 238 (2007).

[55] G. Heinzel, A. Rüdiger, and R. Schilling, Technical Report (2002), https://pure.mpg.de/pubman/faces/ViewItemOverviewPage.jsp?itemId=item_152164.

[56] M. S. Turner, Phys. Rev. D **42**, 3572 (1990).

[57] J. W. Foster, N. L. Rodd, and B. R. Safdi, Phys. Rev. D **97**, 123006 (2018).

[58] A. V. Gramolin, A. Wickenbrock, D. Aybas, H. Bekker, D. Budker, G. P. Centers, N. L. Figueroa, D. F. J. Kimball, and A. O. Sushkov, Phys. Rev. D **105**, 035029 (2022).

[59] T. A. Wagner, S. Schlamminger, J. H. Gundlach, and E. G. Adelberger, Classical Quantum Gravity **29**, 184002 (2012).

[60] Y. Su, B. R. Heckel, E. G. Adelberger, J. H. Gundlach, M. Harris, G. L. Smith, and H. E. Swanson, Phys. Rev. D **50**, 3614 (1994).

[61] P. G. Nelson, D. M. Graham, and R. D. Newman, Phys. Rev. D **42**, 963 (1990).

[62] N. Arkani-Hamed, A. Delgado, and G. F. Giudice, Nucl. Phys. **B741**, 108 (2006).

[63] L. Di Luzio, F. Mescia, and E. Nardi, Phys. Rev. Lett. **118**, 031801 (2017).

[64] K. Agashe, R. Contino, L. Da Rold, and A. Pomarol, Phys. Lett. B **641**, 62 (2006).

[65] E. Fuchs, M. Losada, Y. Nir, and Y. Viernik, J. High Energy Phys. 05 (2020) 056.

[66] N. Arkani-Hamed and K. Harigaya, J. High Energy Phys. 09 (2021) 025.

[67] R. Balkin, C. Delaunay, M. Geller, E. Kajomovitz, G. Perez, Y. Shpilman, and Y. Soreq, Phys. Rev. D **104**, 053009 (2021).

[68] G. ‘t Hooft, NATO Sci. Ser. B **59**, 135 (1980).

[69] D. Antypas, O. Tretiak, A. Garcon, R. Ozeri, G. Perez, and D. Budker, Phys. Rev. Lett. **123**, 141102 (2019).